Materials Transactions, Vol. 43, No. 11 (2002) pp. 2890 to 2896

Solidification Path and Solute Redistribution of an Iron-Based Multi-Component Alloy with Solute Diffusion in the Solid *

Toshiaki Himemiya[1] and Waldemar Wołczyński[2]

[1]*Wakkanai Hokusei College, Wakkanai 097-0013, Japan*
[2]*Institute of Metallurgy and Materials Science, Polish Academy of Sciences, 30-059 Crakow, Reymonta St. 25, Poland*

The micro-segregation of an iron-based multi-component alloy, where the liquid is assumed to be completely mixed and finite diffusion works in the solid, is calculated by a simple method. With this method, not only the solidification path in which the solute distribution ratios change as functions of the composition, but also the solute redistribution profile after solidification can be estimated. As examples, the solidification path and solute redistribution for an iron-carbon-nickel system and an iron-carbon-chromium system have been estimated and compared with the predictions given by assumptions of the equilibrium solidification for carbon and Scheil-type solidification for the metallic solute.

(Received June 17, 2002; Accepted September 27, 2002)

Keywords: *micro-segregation, solidification path, solute redistribution, complete mixing in the liquid, finite diffusion in the solid, analytical solution, multi-component alloy, iron, carbon, metallic element*

1. Introduction

Several attempts[1,2] have been made to predict the solidification path of an iron-based multi-component alloy. For most cases in the solidification of an iron-based alloy, we must estimate the segregation of carbon as the first solute, where the diffusion of carbon in the solid has to be considered and the assumption of the equilibrium solidification about carbon is at best a rough approximate assumption. Several models have been proposed for the case in which the liquid is completely mixed and finite diffusion works in the solid.[3–8] In Wołczyński's method[9,10] for back-diffusion phenomenon during the crystal growth the mass balance problem at the solid-liquid interface is separately treated from the solute redistribution in the solid. Therefore, by using this method, we can easily calculate the solidification path of a multi-component alloy such as Fe–C–X alloy. In Fe–C–X alloys, carbon is an interstitial solute element, while X (a metallic element) is usually a substitutional solute element, and their diffusivities in the solid are more than 3 orders different from each other. For this reason, full numerical methods are often used[1] to calculate the solidification path of an iron-based multi-component alloy. Wołczyński's method makes it easier. Moreover, by using this method,[9,10] we can estimate solute redistribution profiles at each stage of solidification and/or after solidification satisfying the mass balance of the interface.

2. The Model of Wołczyński and Principle of Calculation

Wołczyński proposed a differential equation between the liquid solute content, C_L, and the fraction of solid, f_S. The author called it the B–F–W equation:

$$(1-k)C_L(f_S;\alpha)df_S = (1-f_S)dC_L(f_S;\alpha) + \alpha k f_S dC_L(f_S;\alpha) \quad (1)$$

where $\alpha = D_S t_f / L^2$ is the non-dimensional parameter of the diffusion in the solid, and k is the distribution ratio of the solute. In the expression of α, D_S is the diffusion coefficient in the solid, t_f the local solidification time and L is half of the dendrite spacing. As the author said, this equation is a certain modification of the analogous equation of the Brody and Flemings theory.[3] The left-hand side of the above equation expresses the solute which is rejected against the liquid at the interface by solute distribution when the solid solidifies over df_S. The first term of the right-hand side is the solute increase in the liquid, and the second term is the solute which is transpoterd by the diffusion in the solid.

In the Wołczyński's model and in the present work, basic assumptions are:

1) complete mixing in the liquid within a volume element,
2) finite diffusion in the solid, and
3) equilibrium at the solid-liquid interface and negligible interface undercooling.

In the paper,[9,10] the α-parameter is interpreted as a ratio of local solidification time, t_f, to diffusion time, t_d, necessary to ensure the homogeneity of the solid, expressed as:

$$t_d = \frac{L^2}{D_S}, \quad (2)$$

and

$$\alpha = \frac{t_f}{t_d}. \quad (3)$$

Thus, the α-parameter must be no less than zero and no more than unity. The question is resolved, that is, what happens if the diffusivity in the solid becomes larger in the Brody-Flemings equation? The B–F–W equation reduces to an equilibrium solidification equation when $\alpha = 1$, and reduces to the Gulliver-Scheil equation when $\alpha = 0$. Equation (1) can be integrated if k is constant as:

$$C_L = C_0(1+\alpha k f_S - f_S)^{\frac{k-1}{1-\alpha k}} \quad \text{when} \quad f_S = 0, \quad C_L = C_0. \quad (4)$$

*This Paper was Presented at the Spring Meeting of Japan Institute of Metals, held in Tokyo, on March 27.

Let's apply the B–F–W equation to predict the solidification path and to estimate the solute redistribution of a multicomponent alloy. The procedure of the calculation of the solidification path and solute redistribution consists of three parts. This method divides the solidification stage into many parts within each of which the distribution ratios can be treated as constant. In other words, we assume that

$$\begin{aligned} &\text{at} \quad 0 \le f_S \le f_{S,1} \qquad k_1 = k_1^0, \quad k_2 = k_2^0, \quad \cdots \\ &\text{at} \quad f_{S,1} \le f_S \le f_{S,2} \quad k_1 = k_1^1, \quad k_2 = k_2^1, \quad \cdots \end{aligned} \tag{5}$$

and so on. In the above equations, the subscript of k means j-th solute element.

First, at each stage of solidification, the procedure calls the the progressive-type equation corresponding to eq. (4) for each solute element, j, as;

$$C_L^j = C'^{,j}(1 + \alpha k_j f_S - f_S)^{\frac{k_j - 1}{1 - \alpha k_j}}, \tag{6}$$

where $C'^{,j}$ is the integral constant and can be estimated for the tradition from the 0th stage to the 1st stage as:

$$\begin{aligned} \log C'^{,j} = \log C_0 - \frac{k_j^1 - 1}{1 - \alpha k_j^1} \log[1 + \alpha k_j^1 f_{S,1} - f_{S,1}] \\ + \frac{k_j^0 - 1}{1 - \alpha k_j^0} \log[1 + \alpha k_j^0 f_{S,1} - f_{S,1}] \end{aligned} \tag{7}$$

and so on. This formation is analogous to that of Mori and Ogi.[12] But in this study, we use the new equation, the solution of the B–F–W equation. We may calculate the liquid solute content by using a finite difference formulation of eq. (1), but with use of an analytical solution we need not worry the convergence problem of the Runge-Kutta method.

Second, before calling the progressive-type formation of the solution of B–F–W equation, we must call the thermodynamic database and get the tie-line (get $k_j s$), because the distribution ratios are the functions of the liquid composition. Moreover, we can include the affect of the solidifying temperature on the diffusivity of solute in the solid by changing α step by step. But in this study the temperature dependence of α was not included.

Third, we can estimate the solute distribution in the solid after solidification and/or at given stage of solidification with the form:

$$\begin{aligned} C_S^\beta(f_S;\, f_S^{final}, \alpha) = C_S(f_S;\alpha) + \beta_1(f_S;\, f_S^{final}) \\ \times \beta_2(f_S^{final}, \alpha) C_L(f_S;\alpha). \end{aligned} \tag{8}$$

Where, $C_S^\beta(f_S;\, f_S^{final}, \alpha)$ is the solute content in the solid at the position f_S when the solidification proceeds to f_S^{final}, while $C_S(f_S;\alpha)$ and $C_L(f_S;\alpha)$ are the content in the solid and the content in the liquid at the solid-liquid interface respectively when the fraction of the solid reaches f_S. This equation assumes $C_S^\beta(f_S;\, f_S^{final}, \alpha)$ is increased from $C_S(f_S;\alpha)$ by the solute redistribution with the amount of $\beta_1(f_S;\, f_S^{final})\beta_2(f_S^{final}, \alpha)C_L(f_S;\alpha)$. The expressions of β_1 and β_2 are introduced based on physical consideration.[9,10] In the above equation, β_1 is the coefficient of the extent of solute redistribution in the solid, and β_2 is the intensity of the solute redistribution in the solid. Figure 1 shows the

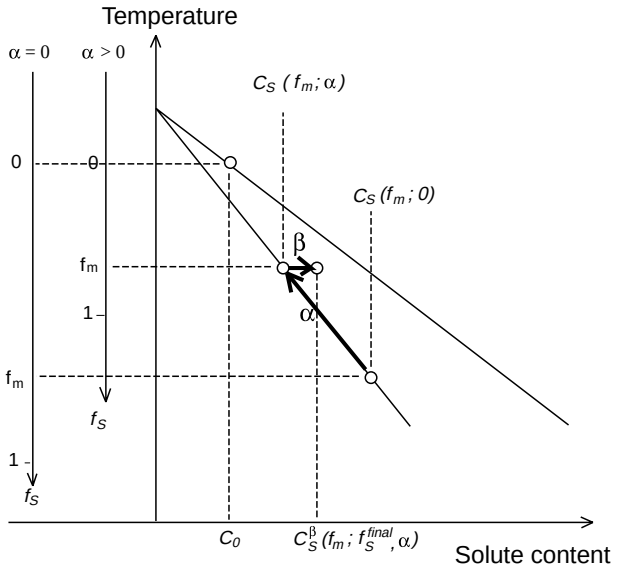

Fig. 1 Physical interpretation of the coefficient, $\beta(f_S;\, f_S^{final}, \alpha)$; f_m is any considered value of the crystal amount.

physical interpretation of the coefficient of solute redistribution $\beta(f_S;\, f_S^{final}, \alpha)$, that is $\beta_1(f_S;\, f_S^{final})\beta_2(f_S^{final}, \alpha)$. The solute content in the solid at the solid-liquid interface is usually lower than that of the no-diffusion case, which might be called the α-effect, but the solute content in the solid ought to be enriched due to diffusion in the solid (solute redistribution) when solidification proceeds to f_S^{final}. The latter might be called the β-effect. β_1 can be estimated by predicting the equilibrium solidification path of the alloy, because β_1 is not affected by α. If we substitute $\alpha = 1$ into eq. (8) that is, we consider the equilibrium solidification, the equation below can be obtained:

$$\begin{aligned} C_S(f_S;1) + \beta_1(f_S;\, f_S^{final})\beta_2(f_S^{final}, 1) C_L(f_S;1) \\ = C_S(f_S^{final}, 1), \end{aligned} \tag{9}$$

where $C_S^\beta(f_S;\, f_S^{final}, 1) = C_S(f_S^{final}, 1)$. As we can assume $\beta_2(f_S^{final}, 1) = 1$ from the intensity of the solute redistribution, then we get:

$$\beta_1(f_S;\, f_S^{final}) = \frac{C_S(f_S^{final};1) - C_S(f_S;1)}{C_L(f_S;1)}. \tag{10}$$

β_2 can be defined by introducing the total mass balance of the solute:

$$\int_0^{f_S^{final}} C_S^\beta(f_S;\, f_S^{final}, \alpha) df_S + (1 - f_S^{final}) C_L(f_S^{final}, \alpha) = C_0. \tag{11}$$

Substituting the definitions of C_S^β and β_1 into eq. (11), the following equation can be obtained:

$$\begin{aligned} &\int_0^{f_S^{final}} C_S(f_S;\alpha) df_S \\ &+ \beta_2(f_S^{final}, \alpha) \int_0^{f_S^{final}} \beta_1(f_S;\, f_S^{final}) C_L(f_S;\alpha) df_S \end{aligned}$$

$$+(1 - f_S^{final})C_L(f_S^{final}; \alpha) = C_0. \quad (12)$$

The above formation can be calculated for each solute element. As is mentioned in introduction of this paper, we can calculate solute distribution profiles at each stage of solidification, but for practical purposes it would be sufficient to estimate the solute distribution profile just after solidification or just after the liquid reaches the eutectic line.

To estimate the solidification path and solute redistribution, the thermo-dynamic database may be called by using Thermo-Calc, but in this work it was done by calling a subroutine made by using Thermo-Calc prior to running the main program.

In Fig. 2, the flow chart to calculate the solidification path and the solute redistribution is shown. To estimate the values of β_1 and β_2, the equilibrium solidification is calculated concurrently with the definite value case of α.

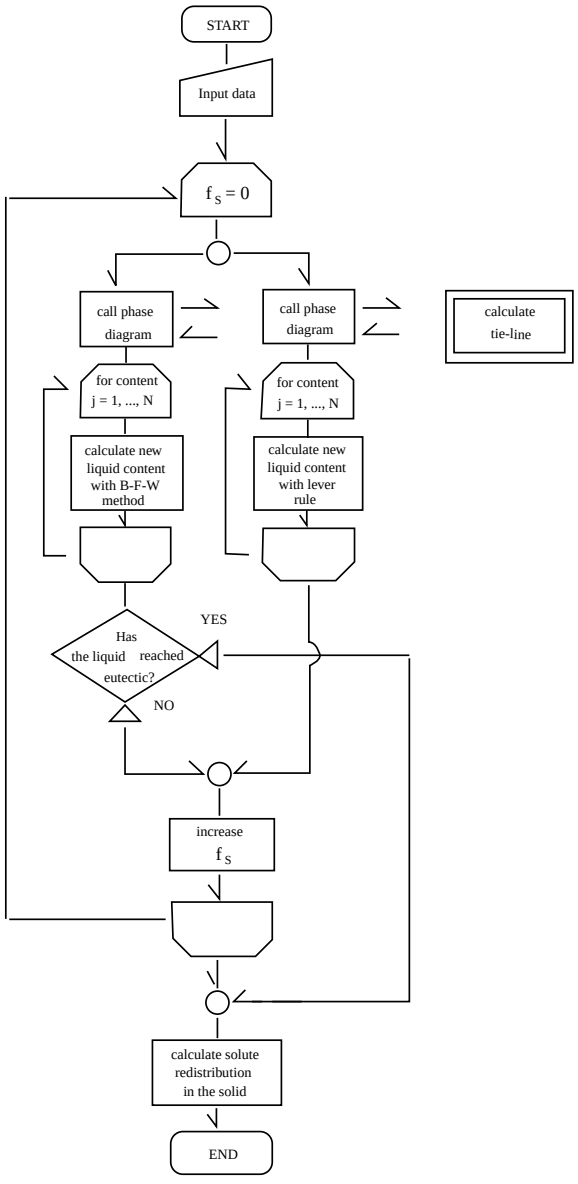

Fig. 2 Flow chart of calculation.

3. Accuracy Estimate

3.1 Sensitivity of the calculated results to the total number of the divisions of the growing crystals

In this method, as we calculate the solidification path by dividing the growing crystals into a number of pieces, it is meaningful to estimate the effect of the number of the total divisions on the calculated result. We calculated the solidification path and solute redistribution of several alloy cases with the number of divisions as 10^2, 10^3, 10^4, 10^5, 10^6 and 10^7, and within the 10^4 to 10^6 range the results varied little. Therefore the demonstration shown below is given with 10^5 divisions. Needless to say this estimate is sensitive to the variation of the distribution coefficients and the accuracy of their data.

3.2 Comparison with other methods

It is also meaningful to compare the results of this method in a simple binary system with the results of the Gulliver-Scheil model,[11] the lever-rule, Kobayashi's solution[6] and the Brody-Flemings solution,[3] because the Gulliver-Scheil model and the lever-rule (equilibrium) are the limit cases of the diffusivity in the solid.

For this purpose, calculations are performed for a simple binary system, in which $k = 0.5$, constant and $\alpha = 0.1$ or $\alpha = 0.01$. The liquid compositions normalized by the initial composition are shown in Fig. 3; also, the results using the Gulliver-Scheil model and the lever-rule are shown. From this figure it can be seen that our results are sandwiched between the Gulliver-Scheil model and the lever-rule. (The result of

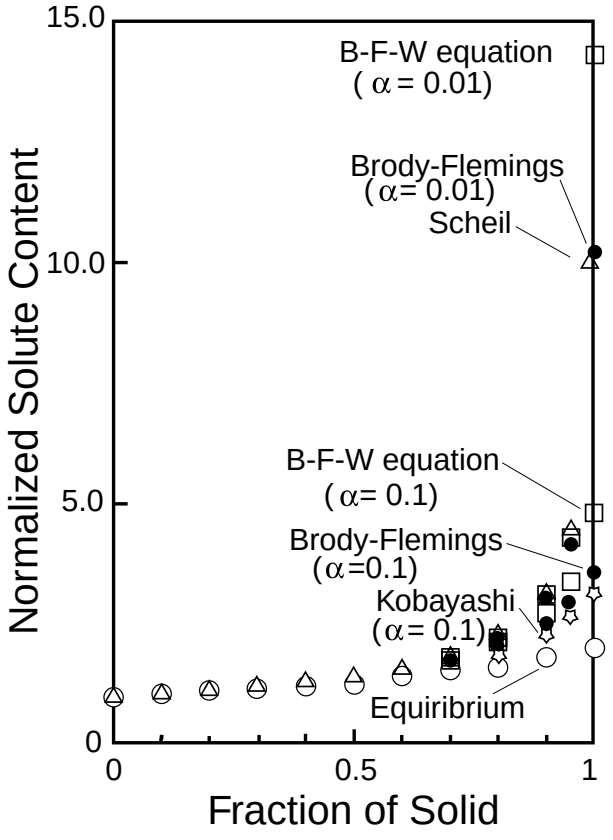

Fig. 3 Comparison for a simple binary system.

Gulliver-Scheil model for $f_S = 1$ is not shown in this figure, because $C_L/C_0 = \infty$. The nearest result to the right frame is for $f_S = 0.99$.) This proves the validity of the physical limitation of the back-diffusion parameter ($0 \leq \alpha \leq 1$). Furthermore, at the final stage of the solidification, the compositions of ours for $\alpha = 0.01$ are greater than that for $\alpha = 0.1$. This result is physically justified. The differences between ours, Brody-Flemings and Kobayshi's are small.

3.3 Accuracy of the estimate of solute redistribution after solidification

If we use the progressive-type formulation of eq. (4), β_1-s and β_2-s ought to be estimated numerically in the node points of the crystal. And the estimate of β-s may affect the accuracy of the estimate of solute redistribution after solidification. Therefore, the estimate of the solute redistribution was compared to the results of the full analytical calculation for a simple binary case of $k = 0.5$ and $\alpha = 0.1$ or $\alpha = 0.01$. With the total divisions number of 10^5 for the growing crystal and total node number of 10^3 for the estimate of β-s, that is, dividing the crystals into 1000 pieces for numerical integration, the error of the estimated solute content was less than 0.052% for $\alpha = 0.01$. For the case of $\alpha = 0.1$, the error was smaller. Such errors can be neglected.

4. Preliminary Arrangement of the Program to Calculate Tie-lines

Before writing the `main` program, the program to calculate tie-lines has to be prepared. In the present case, Fe–C–Ni alloy and Fe–C–Cr alloy are considered. Fe–C–Ni alloy is a typical sample of cast steel. To calculate the solidus composition (C_S^C, C_S^{Ni}) from the liquidus composition (C_L^C, C_L^{Ni}), several isothermal sections of the phase diagram were calculated with Thermo-Calc, and a linear approximation was used between the calculated temperatures. Figure 4 illustrates the principle. Between the temperatures $T_L = T_1$ and $T_L = T_2$ the liquidus composition expressed by the hatched triangle area corresponds to the solidus composition expressed by the same-hatched area. This is an elementary algebraic problem, and we can produce this type of program automatically from the data.

We also considered the Fe–C–Cr alloy in order to consider the solidification path of high-chromium cast iron. In this case, which eutectic will solidify at the final stage is an interesting question.

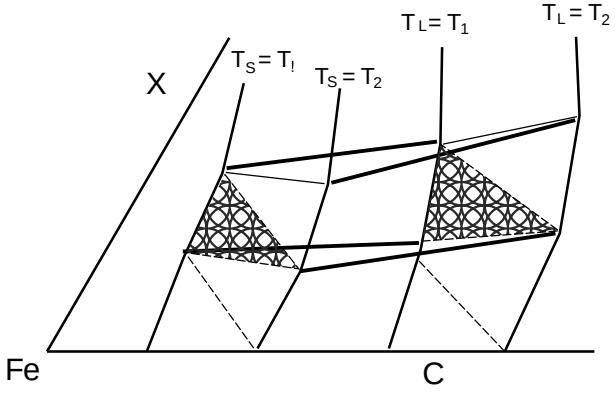

Fig. 4 Preliminary arrangement of the program to calculate tie-lines.

5. A Demonstration for Fe–C–Ni and Fe–C–Cr Alloy and Discussion

In Fig. 5, the calculated solidification path using the present method is shown. In Figs. 5, 7 and 9, the numerals in the figures are the fractions of the solid. The α-parameters are assumed as $\alpha_C = 0.1$ and $\alpha_{Ni} = 0.00002$. The calculated solidification path with complete diffusion for carbon and no diffusion for nickel is also shown in the same figure denoted by Lever + Scheil. The initial compositions are 0.015 mole fraction carbon and 0.07 mole fraction nickel, that is, 0.325 mass% carbon and 7.42 mass% nickel. From this figure, it can be said that the back-diffusion phenomenon causes the difference between the final compositions of the solidification. Also it produces the difference between the solidification paths. The difference becomes larger near the final stage of the solidification (about $f_S > 0.9$) but at the initial and middle stages of the solidification the difference is not large. In Fig. 6, the solute distribution profiles after solidification are shown for the present case. Note that it is predicted in the present calculation that the nickel content will become smaller than the initial content at the final stage. That is because the distribution coefficient for nickel becomes larger than unity along the solidification path at the final stage of the solidification.

In Fig. 7, the calculated solidification paths using the present method and the lever-rule plus Scheil-type soidification are shown for the initial composition of 0.02 mole fraction carbon and 0.1 mole fraction nickel. In this case, the solidification path using the present methods reaches the FCC-cementite eutectic valley when the fraction of solid reaches 0.997. In Fig. 8, the solute distribution profiles just after the eutectic appears in the present method are shown.

In Fig. 9, the solidification paths of 0.045 mole fraction

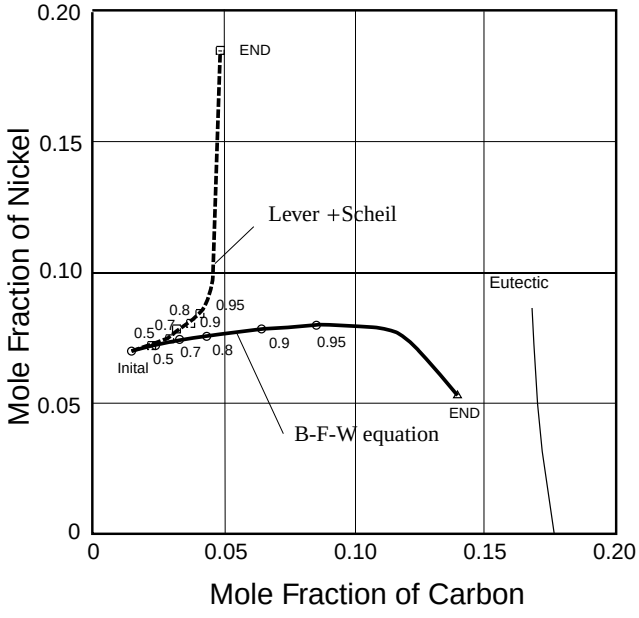

Fig. 5 Solidification paths for Fe–1.5 at%C–7.0 at%Ni alloy.

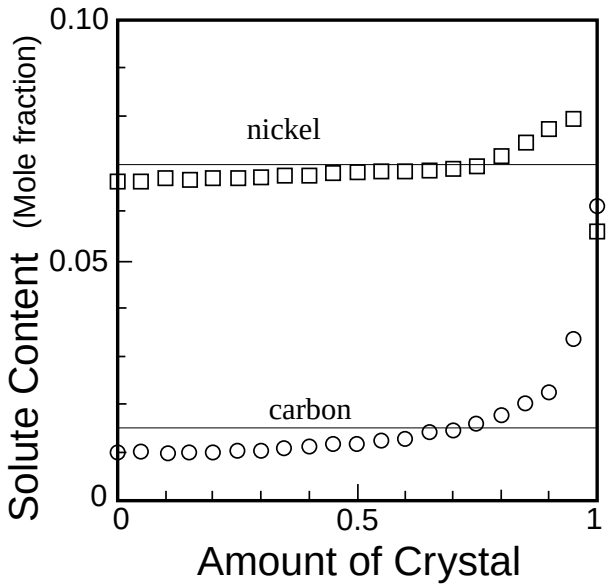

Fig. 6 Solute redistribution profile in the solid for Fe–1.5 at%C–7.0 at%Ni alloy.

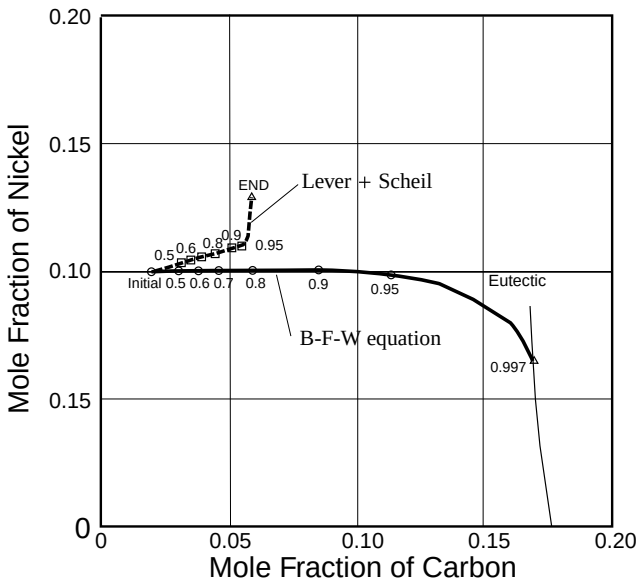

Fig. 7 Solidification paths for Fe–2.0 at%C–10.0 at%Ni alloy.

carbon and 0.092 mole fraction chromium Fe–C–Cr alloy and 0.08 mole fraction carbon and 0.04 mole fraction chromium are drawn. In the method of the present study, the α values of 0.1 for carbon and 0.00003 for chromium are used. For the former case, solidification paths calculated with lever-rule plus Scheil approximation are also drawn. The experimental composition (EPMA)[2)] of the crystallized eutectic is sandwiched between the lever-rule plus Scheil and the present work. Yamamoto and Ogi[2)] reported that the distribution coefficients of chromium and carbon for the experimentally measured data and Thermo-Calc data are somewhat different. We multiplied the correction coefficient by the distribution coefficient from Thermo-Calc to coincide with the coefficient of the measured data, and gained the eutectec contents where the solidification path reaches the eutectic line, 14.4 at% carbon and 18.1 at% chromium; that is, the eutectic predicted

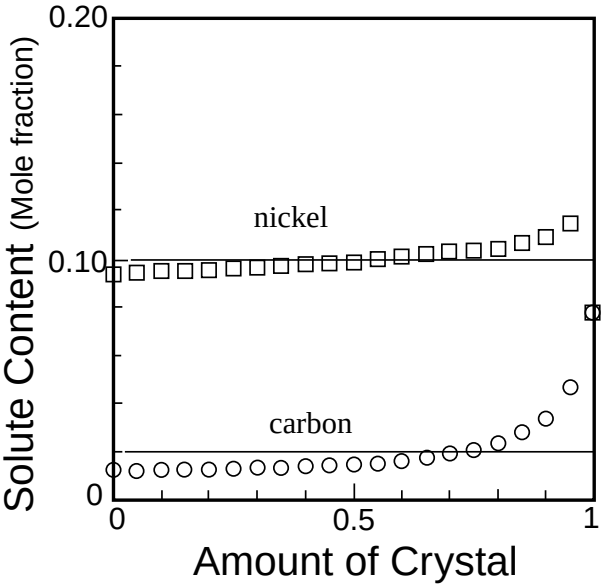

Fig. 8 Solute redistribution profile in the solid for Fe–2.0 at%C–10.0 at%Ni alloy.

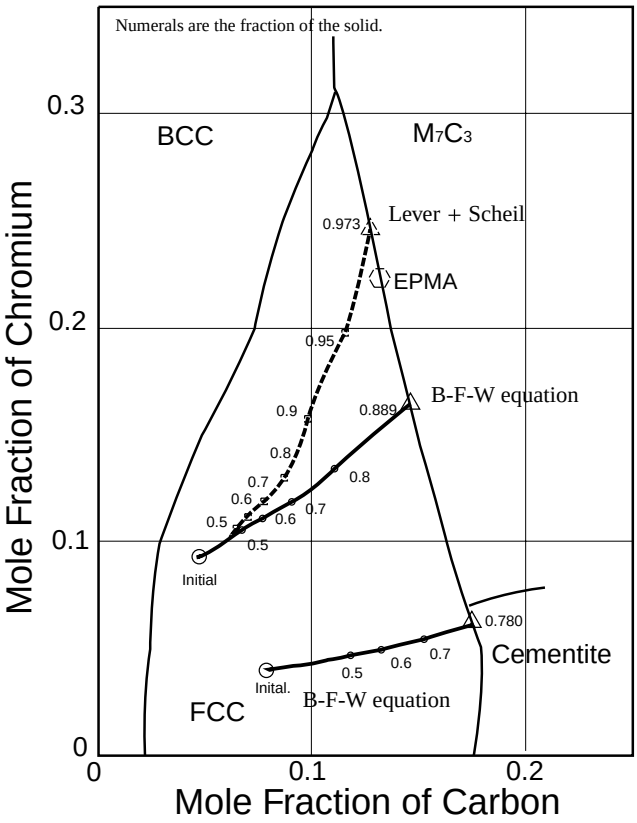

Fig. 9 Solidification paths for Fe–C–Cr alloy.

to crystallize came near to the experimental data. But, this merely means that the accurate distribution coefficient data is important. Moreover, when we increased the α-parameter of carbon to 0.15 using the Thermo-Calc data, the eutectic contents changed to 14.6 at% carbon and 17.1 at% chromium. This also indicates the importance of the estimation of the α-parameter.

By calculation, the Fe–8.0C–4.0Cr alloy will reach the cementite region.

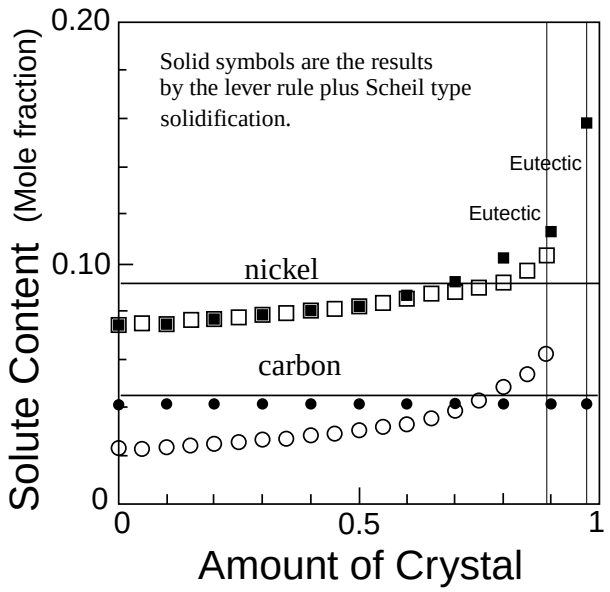

Fig. 10 Solute redistribution profile in the solid for Fe–4.5 at%C–9.2 at%Cr alloy.

In Fig. 10, the estimated solute redistributions for the former case of Fe–C–Cr alloy just after the liquid reaches regions other than FCC phase are drawn. With use of the lever-rule plus Scheil approximation, the carbon content is uniform, while the carbon content in the solid at the last stage increased to twice that of the first solidified part in the present work.

6. Conclusion

The use of the B–F–W equation is useful to calculate the solidification path of a Fe–C–X alloy from the examples of ternary alloys and the results of a simple binary alloy. We can calculate the solidification path and the solute distribution profile after solidification of an iron-carbon-X alloy by using this method.

Acknowledgements

This paper has been prepared in the framework of research project No 7T08B 048 20 supported financially by the State Committee for Scientific Research in Poland.

REFERENCES

1) T. Matsumiya, H. Kajioka, S. Mizoguchi, Y. Ueshima and H. Esaka: *Trans. Iron Steel Inst. Jpn.* **29** (1984) 873–882.
2) K. Yamamoto and K. Ogi: *J. of JFS* **73** (2001) 505–511.
3) H. D. Brody and M. C. Flemings: *Trans. Metall. Soc. AIME* **236** (1966) 615–623.
4) T. W. Clyne and W. Kurz: *Metall. Trans.* **12A** (1981) 965–971.
5) I. Ohnaka: *Trans. Iron Steel Ists. Jpn.* **26** (1986) 1045–1051.
6) S. Kobayashi: *Trans. Iron Steel Ists. Jpn.* **28** (1988) 728–735.
7) T. Himemiya and T. Umeda: *ISIJ Int.* **38** (1998) 730–738.
8) L. Nastac and D. Stefanescu: *Metall. Trans.* **22A** (1993) 2107–2128.
9) W. Wołczyński: *Modelling of Transport Phenomena in Crystal Growth*, (ed. by J. S. Szmyd and K. Suzuki, WIT Press, Southampton-Boston, 2000) pp. 19–59.
10) W. Wołczyński, W. Krajewski, R. Ebner and J. Kloch: *Calphad* **25** (2001) 401–408.
11) E. Scheil: *Z. Metalllk.* **34** (1942) 70–72.
12) N. Mori and K. Ogi: *J. Japan Inst. Metals* **65** (2001) 848–851.

7. Appendix Nomenclatures

Symbol	*Meaning*	*Definition*	*Unit*
C_0	the initial solute content in the liquid		mole fraction
C_L	solute content in the liquid		mole fraction
$C_L(f_S;\alpha)$	solute content in the liquid at the solid-liquid interface when the fraction of the solid is f_S with the non-dimensional diffusion parameter α		mole fraction
C_L^j	content of solute, j, in the liquid		mole fraction
C_S	solute content in the solid		mole fraction
$C_S(f_S;\alpha)$	solute content in the solid at the solid-liquid interface when the fraction of the solid is f_S with the non-dimensional diffusion parameter α		mole fraction
C_S^j	content of solute, j, in the solid		mole fraction
$C_S^\beta(f_S;\ f_S^{final},\alpha)$	solute content in the solid at the position f_S when solidification proceeds to f_S^{final} with the non-dimensional		mole fraction

	diffusion parameter α		
D_S	diffusion coefficient in the solid		$m^2 \cdot s^{-1}$
L	half of the primary dendrite arm spacing		m
T	temperature		K
T_L	liquidus temperature		K
T_S	solidus temperature		K
f_S	fraction of the solid		—
f_S^{final}	fraction of the solid when the solute redistribution is estimated		—
k	distribution ratio of the solute	C_S/C_L	—
k_j	distribution ratio of solute, j	C_S^j/C_L^j	—
t_d	diffusion time necessary to ensure the homogeneity of the solid	L^2/D_S	s
t_f	local solidification time		s
α	non-dimensional parameter of the diffusion in the solid	$D_S t_f/L^2$	—
$\beta(f_S;\ f_S^{final}, \alpha)$	coefficient of solute redistribution within the solid	$\beta_1(f_S;\ f_S^{final})\beta_2(f_S^{final}, \alpha)$	—
$\beta_1(f_S;\ f_S^{final})$	coefficient of extent of solute redistribution within the solid	see eq. (10)	—
$\beta_2(f_S^{final}, \alpha)$	coefficient of intensity of solute redistribution within the solid	see eq. (12)	—